ISTITUTO NAZIONALE DI RICERCA METROLOGICA
Repository Istituzionale

Phase noise cancellation in polarisation-maintaining fibre links

(Article begins on next page)

Phase noise cancellation in polarisation-maintaining fibre links

B. Rauf, M. C. Vélez López, P. Thoumany, M. Pizzocaro, and D. Calonico

Phase noise cancellation in polarisation-maintaining fibre links

B. Rauf,[a)] M. C. Vélez López,[b)] P. Thoumany, M. Pizzocaro, and D. Calonico

Physical Metrology Division, Istituto Nazionale di Ricerca Metrologica (INRIM), Strada delle Cacce 91, 10135 Torino, Italy

The distribution of ultra-narrow linewidth laser radiation is an integral part of many challenging metrological applications. Changes in the optical pathlength induced by environmental disturbances compromise the stability and accuracy of optical fibre networks distributing the laser light and call for active phase noise cancellation. Here we present a laboratory scale optical (at 578 nm) fibre network featuring all polarisation maintaining fibres in a setup with low optical powers available and tracking voltage-controlled oscillators implemented. The stability and accuracy of this system reach performance levels below 1×10^{-19} after 10 000 s of averaging. *Published by AIP Publishing.*
https://doi.org/10.1063/1.5016514

I. INTRODUCTION

Optical fibres are an essential tool of modern metrology and spectroscopy experiments. They offer great flexibility and are able to deliver high mode-qualities and stable polarisation at their output, but also transfer environmental noise, such as seismic/acoustic vibrations or temperature fluctuations, into optical phase noise. This noise can be cancelled out by referencing the fibre output light to the incoming radiation and using this signal to correct the phase and frequency of the light at the output.[1]

Optical fibre links offer the possibility to deliver light of superb stability and accuracy, even across continental distances.[2–4] This allows the transfer of ultra-stable optical radiation between remote locations, enabling radio-astronomy with unprecedented resolution[5] as well as sub-Hz spectroscopy in atomic clocks.[6] Fibre links are also essential parts of high stability measurements of optical frequency ratios as a prerequisite to a redefinition of the second in the International System of Units (SI)[7] and relativistic geodesy,[2,8] as well as the transfer of spectral purity between ultra-stable clock lasers,[9] even across diverse wavelengths.[10]

The most accurate frequency standards to date are optical atomic clocks, reaching uncertainties of a few parts in 10^{18}, although they are not yet realising the definition of the SI-unit the second.[7] Various candidates for a future redefinition are being investigated,[11] while optical clocks are expanding their fields of use to quantum simulations,[12] geodesy and relativity experiments as well as applications,[2,8,13] and the search for variations of fundamental constants.[14,15]

In all optical atomic clocks, an ultra-stable laser interrogates a sub-Hz linewidth optical transition. This laser is usually locked to an ultra-stable reference, such as an ultra-stable cavity. Great efforts are being undertaken to develop cavities reaching thermal noise floor limited stabilities below

1×10^{-16}.[16,17] Such spectral purity is usually preserved throughout the optical path of the laser by phase noise cancelled optical fibre links. Therefore the requirement for these links is to have a stability better than $5 \times 10^{-17} \, \tau^{-1/2}$, as obtained in contemporary performances of optical cavities[16] and optical lattice clocks,[18] and an accuracy below the best clock uncertainty evaluations in the low 10^{-18} region.[7]

At the "Istituto Nazionale di Ricerca Metrologica" (INRIM), an ^{171}Yb optical lattice clock is in operation. The ultra-narrow double-forbidden $^{1}S_0 \rightarrow {}^{3}P_0$ transition is interrogated by a 578 nm laser stabilised to an ultra-stable cavity. A complete description of the experiment can be found in Ref. 19.

Here we report on the phase noise cancellation in a laboratory scale setup at the INRIM facilities distributing the visible ultra-stable laser using polarisation-maintaining (PM) optical fibres. The use of PM fibres is common in laboratory experiments that demand a stable polarisation state of the light, such as high precision atomic spectroscopy, and where power fluctuations arising from polarisation to amplitude noise conversion need to be avoided. With standard single mode fibres, this is commonly achieved by using manual polarisation controls that require to be tweaked as necessary. Yet such a configuration can still be quite susceptible to environmental changes. In our setup, the optical power circulating inside the fibres can be as low as tens of micro-watts. Therefore tracking voltage-controlled oscillators (VCOs) are engaged in the generation of the phase noise error signal, enhancing the robustness of the system. We show that our system meets the demands of state-of-the-art optical clocks and reaches a performance similar to the established single mode fibre links.[20]

II. SETUP

A scheme of the 578 nm dissemination is shown in Fig. 1. The laser itself is situated in a neighbouring laboratory to the Yb lattice clock and is a frequency-doubled 1156 nm diode laser. The total optical power available at 578 nm after the doubling-crystal is about 7 mW. A large part of this power (80%) is sent towards the frequency comb in order to reach a

_____

[a)]Also at Dipartimento di Elettronica e Telecomunicazioni, Politecnico di Torino, Corso Duca degli Abruzzi 24, 10129 Torino, Italy. Electronic mail: b.rauf@inrim.it.

[b)]Also at Real Instituto y Observatorio de la Armada, Calle Cecilio Pujazon, 11100 San Fernando, Cadiz, Spain.
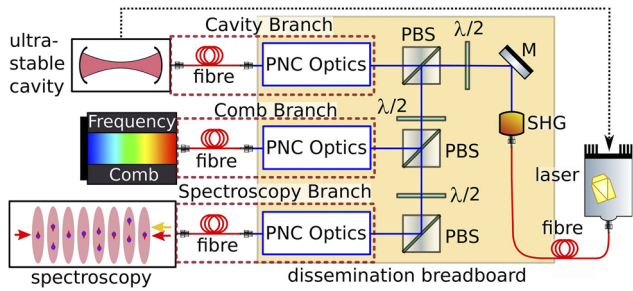
FIG. 1. Dissemination of the 578 nm clock laser. The laser light is distributed to the ultra-stable cavity, the frequency comb, and the atomic spectroscopy by phase-noise cancelled (PNC) fibre links (called branches, inside red dotted boxes). SHG = second harmonic generation, M = mirror, PBS = polarising beam splitter, $\lambda/2$ = half-wavelength retardation plate, blue lines follow the free-space optical path. The black dotted line denotes DC signals of the laser stabilisation to the ultra-stable cavity.
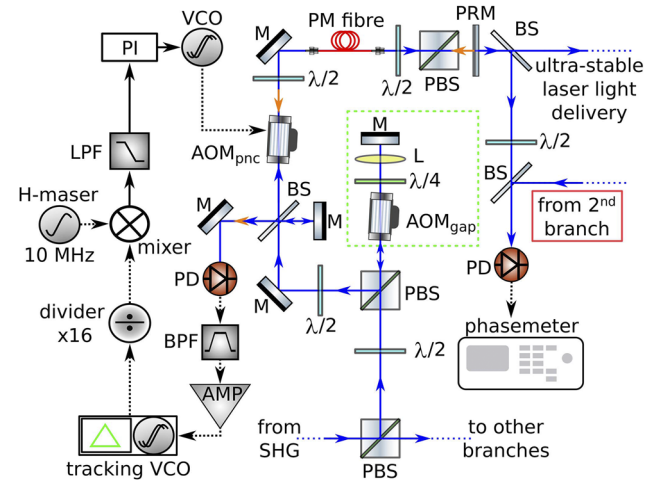

FIG. 2. Sketch of the fibre noise cancellation setup and its assessment. The laser light enters the branch coming from the SHG crystal. The double-pass AOM in cat-eye configuration is marked with green dots. The laser light is signalled with blue arrows, but the retro-reflected beam path is signalled with orange arrows. PD = photodiode, VCO = voltage controlled oscillator, LPF = low-pass filter, AMP = amplifier, BPF = band-pass filter, L = lens, PRM = partial reflecting mirror, PI = proportional-integral controller, BS = power beam splitter.

high signal-to-noise ratio in the beatnote with the comb light. The spectroscopy of the ultra-narrow atomic transition and the ultra-stable cavity on the other hand need only little power, as the light power impinging on the cavity and the Yb atoms is in the μW to nW region. Therefore the fibre noise cancellation system needs to work even with low optical powers (about 100 μW) circulating inside the optical path of the phase noise cancellation system, that is the power in each branch after the polarising beam splitter (PBS) in Fig. 1. A fraction of this power is then available for the generation of the optical phase noise error signal. The laser light is connected to the dissemination breadboard by optical fibres. Any airflow inside the lab is shielded by an acrylic enclosure around the breadboard protecting the free-space optical paths of the setup.

The fast stabilisation of the diode laser to one cavity mode acts upon the laser current and is supported by a low-bandwidth drift compensation controlling the diode laser internal cavity length (piezo-voltage). The performance of the laser stabilised to the ultra-stable cavity is similar to what has been previously reported.[21] After passing through the second harmonic generation (SHG) crystal, the radiation is split into three branches, each leading to a dedicated 20 m PM fibre delivering the light to the ultra-stable cavity, the frequency comb and the atomic spectroscopy within the science chamber of the lattice clock.

These PM fibres are optimised for wavelengths around the Yb clock transition of 578 nm and engineered in the panda style, meaning that a significant fibre birefringence is obtained through stress rods pulling on the core and thereby suppressing cross talk between the fibre polarisation axis. As a consequence, small variations of the fibre birefringence exerted, e.g., by mechanical forces do not lead to significant polarisation noise, unlike the case of single-mode fibres.[22] This attribute allows polarisation cleaning after the fibre without introducing polarisation to amplitude noise conversion.

All of these branches share an identical layout, which is sketched in Fig. 2. The ultra-stable laser light enters the branch coming from the direction of the SHG output, as shown in Fig. 1. At first, a double-pass acousto-optic modulator (AOM_{gap}) in cat-eye configuration[23] is used to bridge the frequency gap between the nearest cavity mode and the atomic resonance. Subsequently a power beam splitter (BS) serves as

the reference point of an imbalanced optical interferometer with the short arm constituting the reference beam (30% of the incoming beam power reflected) for the generation of the phase-noise error signal. Before passing through the 20 m PM fibre (long interferometer arm), the beam is imprinted with an 80 MHz frequency shift by AOM_{pnc}. A half-waveplate is used to align the light polarisation with the slow axis of the PM fibre, minimising polarisation-noise from the fibre. The polarisation extinction ratio at this point is determined by the PBS in the optical path after the cat-eye AOM setup as 100:1 (reflected beam).

After the fibre, the polarisation of the light is cleaned and a part ($\approx$40%) of the radiation is retro-reflected by a partial reflecting mirror. Only the comb-branch features higher optical power, compensated by a reduced reflectivity of the partial reflecting mirror ($\approx$15%). Typically 20 μW of optical power is delivered after the partial reflecting mirror (in the case of the comb branch these are some 1.5 mW). The polarisation is cleaned using a $\lambda/2$ waveplate and a PBS with a polarisation extinction ratio of at least 1000 : 1. A maximised PBS output ensures that also the back-reflected beam is aligned on the slow axis of the PM fibre. This procedure suppresses the amplitude noise in the optical interferometer stemming from the fibre birefringence, which is quite sensitive to temperature changes in the case of panda-style PM fibres.[22] The reflected light passes once again the AOM_{pnc} and then interferes with the reference beam. All our fibres use angle flat connectors (a variation of angle polished connectors manufactured by OZ optics) to reduce back-reflection from the fibre tip. We found that this back-reflection gives rise to a signal 30 dB smaller than the one from the retro-reflector.

We note that having the same polarisation on the retro-reflected beam significantly improves the system performances: in fact, we observed an enhanced sensitivity to polarisation fluctuations when the back-reflected beam had a

rotated polarisation direction with respect to the initial beam. This happens because this beam is then not aligned to a fibre axis and the birefringence is quite sensitive to temperature fluctuations.

The beatnote between the reference and the retro-reflected beam carries the information on the phase noise along the optical path and is found at a frequency of 160 MHz. It is recorded on a fast photodiode (Menlo FPD510-FV, bandwidth 200 MHz), subsequently filtered with a band-pass filter (bandwidth 14 MHz around 157 MHz), and then amplified by 30 dB. This beatnote signal is then tracked by a voltage-controlled oscillator (VCO), which has a bandwidth of 3 MHz. As a result, the reliability of the fibre link is improved since fluctuations in the optical beatnote might cause cycle slips otherwise. The VCO frequency is divided by 16 with a frequency divider and directly compared in a mixer with a 10 MHz reference signal coming from a H-maser. A low-pass filter (bandwidth 500 kHz) subsequently filters out the DC part of this signal. A proportional-integral (PI) controller takes this error signal to feed the frequency of a VCO that in turn drives the AOMpnc in order to cancel all phase noise occurring along the optical and in-fibre path between the BS and the partial reflecting mirror. In order to minimise the residual noise along the optical path, the control bandwidth of the PI is set individually for each fibre noise cancellation to optimised values around 20 kHz.

The radiation delivered by all three branches has the same spectral attributes except for a possible adjustable frequency offset introduced by the double-pass AOM and the intrinsic optical path-length noise of each branch.

The fibre link electronics feature also an "open loop" operation. In this mode, the VCO providing the AOMpnc RF signal at 80 MHz is stabilised with a phase locked loop to the H-maser signal. This operational mode is useful for initial alignment or to keep light delivered through the fibre even when the back-reflected signal is missing.

At last, the part of the beam not retro-reflected after the partial reflecting mirror is used to deliver the ultra-stable radiation to its destination (the ultra-stable cavity, the frequency comb, or the atomic spectroscopy).

The facilities of the Yb lattice clock at INRIM feature an air conditioning system that stabilises the temperature inside the clock laboratory to within a periodic oscillation of 0.2 K amplitude and with a periodicity of 15 min (quasi sinusoidal oscillation), while the airflow alternates its intensity accordingly. This means that the momentary temperature change in the lab can be as high as 0.5 mK s^{-1}. Such temperature oscillations introduce changes in the fibre length and the fibre index of refraction leading to a calculated noise at the half-period time (maximum temperature excursion and applying the sensitivities of pure silica[24]) of about 1×10^{-17} and 1×10^{-16}, respectively.

There is a remaining up to 2 m of free-space optical path in each of the Yb laser branches that is not shared by any other branch and is situated outside of the phase-noise cancellation interferometer. An enclosure made from acrylic glass around the breadboard containing the optics of these branches shields efficiently acoustic noise and short-term density fluctuations, whereas the stiff breadboard ensures that the seismic

noise is common to all optical elements. The dissemination breadboard, which is made from steel, experiences also temperature excursions due to the lab temperature fluctuations. These have the same periodicity as the laboratory temperature, but with a much smaller amplitude of 4 mK. The Doppler shift caused by the steel breadboard temperature fluctuations altering the free-space optical path is estimated at 1×10^{-18} at 450 s.

III. RESULTS

The metrological characterisation of the phase noise cancellation was performed through pairwise evaluations of the fibre links, as shown in Fig. 2. For these measurements, the radiation after the partial reflecting mirror was beat against the light arriving from a 2nd identical setup in a short free-space optical path. These measurements were performed inside a separate acrylic enclosure and the beatnote on a photodiode recorded with a phasemeter or frequency counter.

In a first step, we determined the minimum input light power within one branch (after the PBS in Fig. 1) needed for the phase noise cancellation to function properly to be 90 μW. Below this value, cycle slips appeared in the locking of the tracking oscillator, compromising the stability of the phase noise cancellation.

The possibility of such cycle slips was investigated by looking for jumps by an integer number of 2π in phase in the beatnote between the outputs of the phase noise cancelled fibres. As can be seen from Fig. 3, no cycle slips occurred in 20 h of measurement. All data points were within 0.05 Hz (1 part in 10^{16}).

We compared the noise between two branches with and without the lid of the acrylic enclosure attached in order to determine the influence of turbulent air in the free-space region of the branches on the performance of the phase noise cancellation. The results are shown in Fig. 4. Turbulent air in the free-space paths outside of the phase-noise cancellation loops does increase the phase noise of the disseminated laser light in a region between 0.1 Hz and 10 Hz, which includes
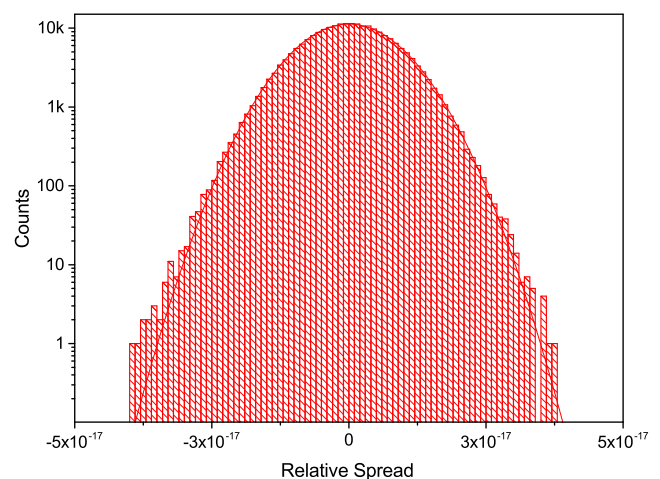
FIG. 3. Histogram of a 20 h measurement looking for cycle slips in the beatnote. No points were recorded outside of the scale used for the abscissa.
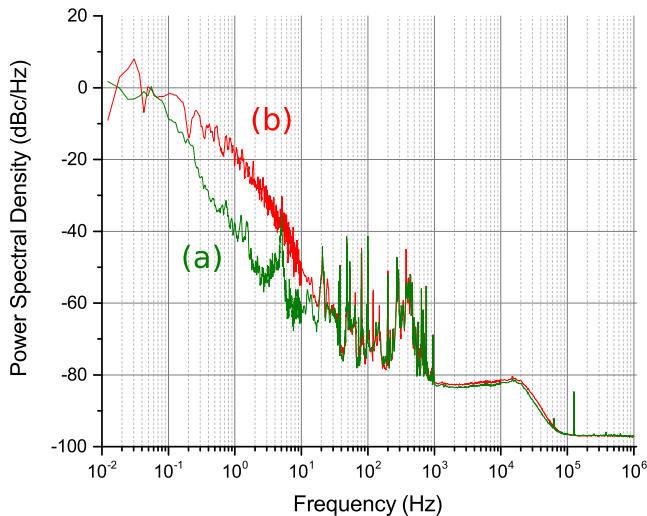
FIG. 4. Power spectral density (PSD) of the beatnote between two branches with (a) and without (b) the lid of the acrylic enclosure attached. The slightly higher phase noise level compared to Fig. 5 is due to different optical and electronic power levels during this measurement. The results are nonetheless transferable to the current setup.

especially the time scale of one clock cycle (0.1 s to 0.5 s) and is therefore most critical. The acrylic enclosure suppresses this effect efficiently.

The power spectral density of a typical phase noise cancellation performance measurement between two branches is shown in Fig. 5. The curve follows a $1/f^2$ behaviour (white frequency noise) in the low frequency region (0.1 mHz–0.1 Hz), succeeded by—typically acoustic—noise displaying pronounced peaks around 10 Hz and between 300 Hz and 500 Hz. Electronic noise stemming from the power line at 50 Hz and harmonics thereof is also visible. A white phase noise pedestal is reached for frequencies between 4 kHz and 20 kHz. The signal-to-noise ratio (SNR) of the beatnote on the detection photodiode (42 dB in 100 kHz) agrees with the measured phase noise ($\approx$−90 dBc/Hz) in this region. At 20 kHz, the

bandwidth of the control is reached, and for higher frequencies, only electronic noise is left in the signal.

The Allan-deviation of the phase noise cancellation performance is shown in Fig. 6. These measurements were obtained using a phasemeter with a bandwidth of 500 Hz and a gate time of 1 ms. The exception is the 4-day measurement that was acquired with a high-resolution K + K FXE counter (Λ-variance) and a gate time of 1 s (the resulting equivalent bandwidth is 0.5 Hz).

The unstabilised fibre link shows an Allan-deviation that is not compatible with state-of-the-art ultra-stable lasers and clock stabilities. Once the fibre noise cancellation is active, the low integration time regime ($\tau < 1$ s) averages down as $1/\tau$, matching white phase noise, as expected for fibre links. At about 4 s, the slope changes towards an overall $\tau^{-1/2}$ trend, revealing white frequency noise. Looking at the 4 day measurement it becomes clear that the noise at time scales $\tau \geq 450$ s is dominated by the periodic noise of the air conditioning system inside the INRIM laboratories.

The Λ-variance of the high resolution counter reduces its sensitivity to white phase noise in comparison to the phasemeter measurements.[25,26] As a consequence, the Allan deviation obtained with the counter measurement is a bit below the phasemeter values for those short time scales where white phase noise dominates. For integration times above a few seconds, the noise is changing to white frequency noise behaviour, and at long time scales, the blue and the red curves agree quite closely, as expected. When taking a phasemeter measurement with a bandwidth of 0.5 Hz, we saw that the blue and red curves do also agree at the 1 s value, but the information on the high frequency behaviour of the fibre link is lost.

In conclusion, we measured a stability of 2×10^{-17} at $\tau = 1$ s that follows a $7 \times 10^{-18}\ \tau^{-1/2}$ behaviour for longer time scales ($\tau \geq 1000$ s), as shown in Fig. 6. The phase noise
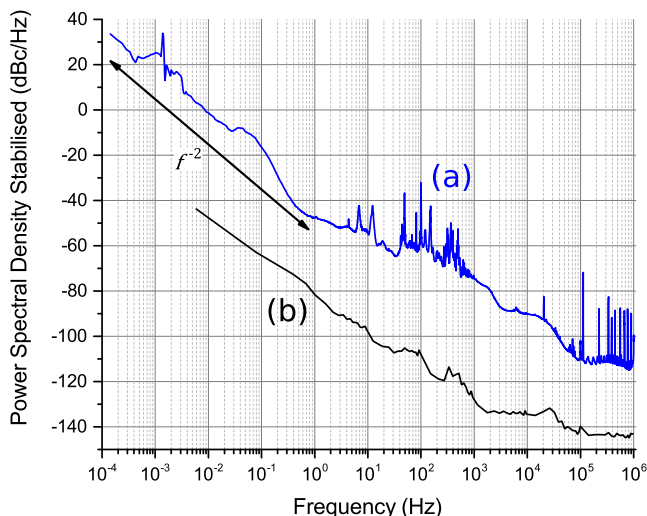

FIG. 5. Power spectral density of the beatnote between the output laser radiation of two phase-noise cancelled fibre links, measured with a Microsemi 5125 A phasemeter (a) and noise floor of the phasemeter (b).
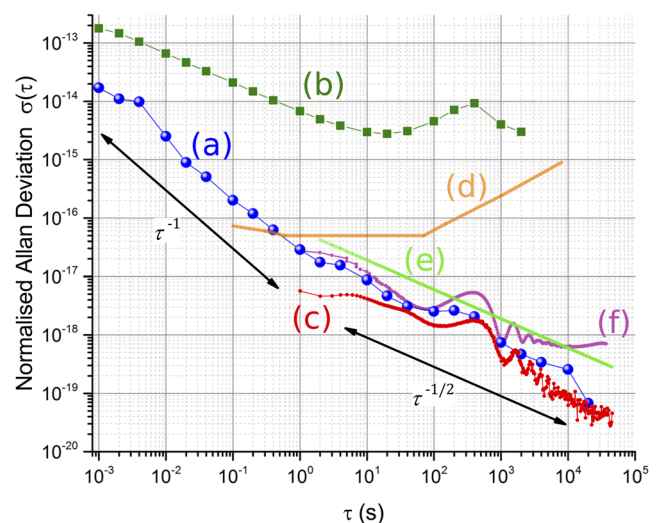

FIG. 6. Allan-deviation of the same measurement as in Fig. 5 (a), compared with measurements of the unstabilised link performance (b) and a 4-day long assessment of the fibre link performance (c). The best reported stabilities of an optical cavity[16] (d) and of an ensemble of optical lattice clocks[18] (e) are shown as benchmarks. The magenta curve (f) displays the total Allan-deviation obtained when using a mismatched polarisation for the back-reflected beam. Lines between measurement points are there to guide the eye.

cancelled fibre link has a higher stability than the benchmark curves representing the latest performances of ultra-stable lasers[16] and optical clock ensembles.[18] The resulting uncertainty of 5×10^{-20} is limited only by statistics. No frequency offset in the beatnote between the pairwise investigation of the fibre links was detected.

The fibre noise cancellation system presented here maintains the same polarisation throughout the reference- and the back-reflected beam. If the polarisation of the back-reflected beam was intentionally not aligned with the fibre axis by approximately $45°$, we observed a noise floor in the Allan-deviation at 6×10^{-19} (magenta curve).

IV. DISCUSSION

We have successfully developed and characterised a fibre noise cancellation system designed to tackle the need of spectral purity transfer of an ultra-stable laser at 578 nm using circulating optical powers below 100 μW. The assessed fibre link uncertainty of 5×10^{-20} and stability of $7 \times 10^{-18}\ \tau^{-1/2}$ surpass the best contemporary lasers stabilised to an ultra-stable cavity,[16] as well as the highest demonstrated stability and accuracy of an optical clock so far.[7,18]

The periodic change of temperature acting on the length of the optical path between the fibre noise cancellation units leads to an uncertainty in the low 10^{-18} region at 450 s, in agreement with our predictions. The temperature change follows a somewhat sinusoidal curve and therefore, for time scales $\tau \gg 450$ s, turns into a white frequency noise behaviour, averaging down as $\tau^{-1/2}$.

The performance we measured is suitable for the transfer of high-purity laser radiation and for the state of the art optical clocks. If desired, it could still be diminished by a reduction of the optical path between the dissemination branches (Fig. 1), to the point of using the same reference mirror for all fibre links (calling for a sophisticated electronic setup), or by thermally insulating the steel breadboard supporting the whole free-space optics of the laser dissemination and the fibre noise cancellation systems.

[1]L.-S. Ma, P. Jungner, J. Ye, and J. L. Hall, "Delivering the same optical frequency at two places: Accurate cancellation of phase noise introduced by an optical fiber or other time-varying path," Opt. Lett. **19**, 1777–1779 (1994).

[2]C. Lisdat, G. Grosche, N. Quintin, C. Shi, S. Raupach, C. Grebing, D. Nicolodi, F. Stefani, A. Al-Masoudi, S. Dörscher, S. Häfner, J.-L. Robyr, N. Chiodo, S. Bilicki, E. Bookjans, A. Koczwara, S. Koke, A. Kuhl,

F. Wiotte, F. Meynadier, E. Camisard, M. Abgrall, M. Lours, T. Legero, H. Schnatz, U. Sterr, H. Denker, C. Chardonnet, Y. Le Coq, G. Santarelli, A. Amy-Klein, R. Le Targat, J. Lodewyck, O. Lopez, and P.-E. Pottie, "A clock network for geodesy and fundamental science," Nat. Commun. **7**, 12443 (2016).

[3]D. Calonico, E. K. Bertacco, C. E. Calosso, C. Clivati, G. A. Costanzo, M. Frittelli, A. Godone, A. Mura, N. Poli, D. V. Sutyrin, G. Tino, M. E. Zucco, and F. Levi, "High-accuracy coherent optical frequency transfer over a doubled 642-km fiber link," Appl. Phys. B **117**, 979–986 (2014).

[4]A. Matveev, C. G. Parthey, K. Predehl, J. Alnis, A. Beyer, R. Holzwarth, T. Udem, T. Wilken, N. Kolachevsky, M. Abgrall, D. Rovera, C. Salomon, P. Laurent, G. Grosche, O. Terra, T. Legero, H. Schnatz, S. Weyers, B. Altschul, and T. W. Hänsch, "Precision measurement of the hydrogen $1s$–$2s$ frequency via a 920-km fiber link," Phys. Rev. Lett. **110**, 230801 (2013).

[5]C. Clivati, R. Ambrosini, T. Artz, A. Bertarini, C. Bortolotti, M. Frittelli, F. Levi, A. Mura, G. Maccaferri, M. Nanni, M. Negusini, F. Perini, M. Roma, M. Stagni, M. Zucco, and D. Calonico, "A VLBI experiment using a remote atomic clock via a coherent fibre link," Sci. Rep. **7**, 40992 (2017).

[6]M. Takamoto, I. Ushijima, N. Das, N. Nemitz, T. Ohkubo, K. Yamanaka, N. Ohmae, T. Takano, T. Akatsuka, A. Yamaguchi, and H. Katori, "Frequency ratios of Sr, Yb, and Hg based optical lattice clocks and their applications," C. R. Phys. **16**, 489–498 (2015), the measurement of time/La mesure du temps.

[7]P. Gill, "Is the time right for a redefinition of the second by optical atomic clocks?," J. Phys.: Conf. Ser. **723**, 012053 (2016).

[8]T. Takano, M. Takamoto, I. Ushijima, N. Ohmae, T. Akatsuka, A. Yamaguchi, Y. Kuroishi, H. Munekane, B. Miyahara, and H. Katori, "Geopotential measurements with synchronously linked optical lattice clocks," Nat. Photonics **10**, 662–666 (2016).

[9]T. Akatsuka, H. Ono, K. Hayashida, K. Araki, M. Takamoto, T. Takano, and H. Katori, "30-km-long optical fiber link at 1397 nm for frequency comparison between distant strontium optical lattice clocks," Jpn. J. Appl. Phys., Part 1 **53**, 032801 (2014).

[10]S. Falke, N. Lemke, C. Grebing, B. Lipphardt, S. Weyers, V. Gerginov, N. Huntemann, C. Hagemann, A. Al-Masoudi, S. Häfner, S. Vogt, U. Sterr, and C. Lisdat, "A strontium lattice clock with 3×10^{-17} inaccuracy and its frequency," New J. Phys. **16**, 073023 (2014).

[11]A. D. Ludlow, M. M. Boyd, J. Ye, E. Peik, and P. O. Schmidt, "Optical atomic clocks," Rev. Mod. Phys. **87**, 637–701 (2015).

[12]L. F. Livi, G. Cappellini, M. Diem, L. Franchi, C. Clivati, M. Frittelli, F. Levi, D. Calonico, J. Catani, M. Inguscio, and L. Fallani, "Synthetic dimensions and spin-orbit coupling with an optical clock transition," Phys. Rev. Lett. **117**, 220401 (2016).

[13]A. Bjerhammar, "On a relativistic geodesy," Bull. Géod. **59**, 207–220 (1985).

[14]S. Blatt, A. D. Ludlow, G. K. Campbell, J. W. Thomsen, T. Zelevinsky, M. M. Boyd, J. Ye, X. Baillard, M. Fouché, R. Le Targat, A. Brusch, P. Lemonde, M. Takamoto, F.-L. Hong, H. Katori, and V. V. Flambaum, "New limits on coupling of fundamental constants to gravity using ^{87}Sr optical lattice clocks," Phys. Rev. Lett. **100**, 140801 (2008).

[15]R. M. Godun, P. B. R. Nisbet-Jones, J. M. Jones, S. A. King, L. A. M. Johnson, H. S. Margolis, K. Szymaniec, S. N. Lea, K. Bongs, and P. Gill, "Frequency ratio of two optical clock transitions in ^{171}Yb$^+$ and constraints on the time variation of fundamental constants," Phys. Rev. Lett. **113**, 210801 (2014).

[16]D. G. Matei, T. Legero, S. Häfner, C. Grebing, R. Weyrich, W. Zhang, L. Sonderhouse, J. M. Robinson, J. Ye, F. Riehle, and U. Sterr, "1.5 μm lasers with sub-10 mHz linewidth," Phys. Rev. Lett. **118**, 263202 (2017).

[17]S. Häfner, S. Falke, C. Grebing, S. Vogt, T. Legero, M. Merimaa, C. Lisdat, and U. Sterr, "8×10^{-17} fractional laser frequency instability with a long room-temperature cavity," Opt. Lett. **40**, 2112–2115 (2015).

[18]M. Schioppo, R. C. Brown, W. F. McGrew, N. Hinkley, R. J. Fasano, K. Beloy, T. H. Yoon, G. Milani, D. Nicolodi, J. A. Sherman, N. B. Phillips, C. W. Oates, and A. D. Ludlow, "Ultrastable optical clock with two cold-atom ensembles," Nat. Photonics **11**, 48–52 (2016).

[19]M. Pizzocaro, P. Thoumany, B. Rauf, F. Bregolin, G. Milani, C. Clivati, G. A. Costanzo, F. Levi, and D. Calonico, "Absolute frequency measurement of the $^1S_0 \rightarrow ^3P_0$ transition of 171Yb," Metrologia **54**, 102 (2017).

[20]G. Grosche, "Eavesdropping time and frequency: Phase noise cancellation along a time-varying path, such as an optical fiber," Opt. Lett. **39**, 2545–2548 (2014).

[21] M. Pizzocaro, G. A. Costanzo, A. Godone, F. Levi, A. Mura, M. Zoppi, and D. Calonico, "Realization of an ultrastable 578-nm laser for an Yb lattice clock," IEEE Trans. Ultrason., Ferroelectr. Freq. Control **59**, 426–431 (2012).

[22] J. Noda, K. Okamoto, and Y. Sasaki, "Polarization-maintaining fibers and their applications," J. Lightwave Technol. **4**, 1071–1089 (1986).

[23] E. A. Donley, T. P. Heavner, F. Levi, M. O. Tataw, and S. R. Jefferts, "Double-pass acousto-optic modulator system," Rev. Sci. Instrum. **76**, 063112 (2005).

[24] T. Toyoda and M. Yabe, "The temperature dependence of the refractive indices of fused silica and crystal quartz," J. Phys. D: Appl. Phys. **16**, L97 (1983).

[25] S. T. Dawkins, J. J. McFerran, and A. N. Luiten, "Considerations on the measurement of the stability of oscillators with frequency counters," IEEE Trans. Ultrason., Ferroelectr. Freq. Control **54**, 918–925 (2007).

[26] C. E. Calosso, C. Clivati, and S. Micalizio, "Avoiding aliasing in Allan variance: An application to fiber link data analysis," IEEE Trans. Ultrason., Ferroelectr. Freq. Control **63**, 646–655 (2016).